Laser Physics

PAPER

Laser wavelength effect on nanosecond laser light reflection in ablation of metals

IOP Publishing | Astro Ltd Laser Physics
Laser Phys. 26 (2016) 126101 (6pp) doi:10.1088/1054-660X/26/12/126101

Laser wavelength effect on nanosecond laser light reflection in ablation of metals

O Benavides[1], L de la Cruz May[1], E B Mejia[2], J A Ruz Hernandez[1] and A Flores Gil[1]

[1] Universidad Autónoma del Carmen, Cd. del Carmen, Campeche, Mexico
[2] Centro de Investigaciones en Óptica, León, Guanajuato, Mexico

E-mail: obenavides@pampano.unacar.mx

Received 16 August 2016, revised 24 October 2016
Accepted for publication 30 October 2016
Published 16 November 2016

Abstract

Reflection of nanosecond laser pulses with different wavelengths (1.06 and 0.69 μm) in ablation of titanium in air is studied experimentally. The laser wavelength effect on reflection is essential at low laser fluence values. However, it becomes negligible for laser fluence values by about an order of magnitude higher than the plasma ignition threshold. We speculate that the disappearance of the wavelength effect is explained by counter-acting processes of the laser light absorption in plasma, which increases with laser wavelength, and absorption in the surface layer, which decreases with increasing laser wavelength.

Keywords: laser ablation, nanosecond laser, reflection, laser plasmas, titanium

(Some figures may appear in colour only in the online journal)

1. Introduction

Nanosecond laser ablation of solids [1–4] has found applications in many areas, including nano/microprocessing of materials [5–9], thin film deposition [10], modification of optical properties [11, 12], laser-induced breakdown spectroscopy [13, 14], modification of wetting properties [15, 16], laser marking [17], biomedicine [18], producing diamond-like materials [19], and others. Despite the numerous applications, the physical processes underlying ablation are not yet fully understood. In particular, reflection/absorption of high-intensity nanosecond laser pulses in ablation of metals is one of these processes. Previous experiments on reflection of nanosecond laser pulses have shown a significant reflectivity drop associated with plasma ignition near the sample surface [20–25]. In a number of applications, for example, in inductively coupled plasma mass spectrometry (ICP-MS) [26], there is the need in understanding laser-beam wavelength effects in nanosecond laser ablation. Here, to further advance understanding the reflection process in ablation of metals, we perform a comparative experimental study on the reflection of nanosecond laser pulses with different wavelength (1.06 and 0.69 μm) under the same other experimental conditions. The studied metal is titanium. Our choice of titanium is motivated by its various biomedical applications [27]. We find that the laser wavelength effect is essential at low laser fluence values, while it becomes negligible for laser fluence values exceeding the plasma formation threshold by about an order of magnitude.

2. Experimental setup

Figure 1 shows the experimental setup used to study laser light reflection. An Nd:YAG laser with $\lambda = 1.06$ μm and a ruby laser with $\lambda = 0.69$ μm are used for ablation. The pulse duration of both lasers is 50 ns at FWHM (full width at a half-maximum intensity). The laser fluence incident on the sample is varied by a calibrated variable attenuator. The laser beam is focused onto the sample using a lens with a focal distance of 250 mm. To study reflection, we use a hemiellipsoidal light reflector technique introduced in [22, 28], which provides collecting both specular and diffuse components of the reflected light. The collection of both these components is critically important because the sample surface becomes damaged during the nanosecond laser pulse, resulting in scattering the reflected light.

The sample is placed in the internal focal point of the hemiellipsoidal reflector. To reduce laser light backscattering through the entrance hole in the hemiellipsoidal reflector, the sample is tilted at 19° relative to the laser beam axis. The laser

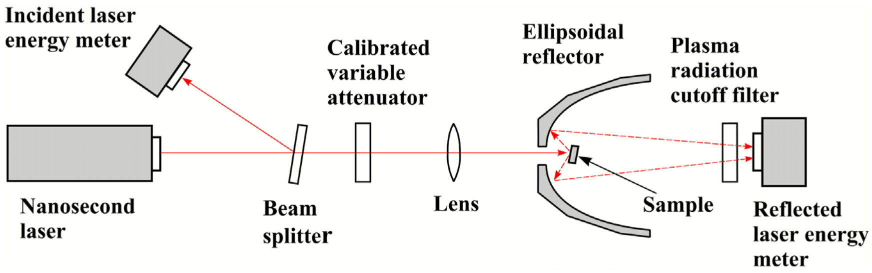

Figure 1. Experimental setups for studying laser light reflection in ablation of titanium.

light reflected by the sample is collected in the external focal point of the reflector and its energy, E_{refl}, is measured with an energy meter. To prevent plasma radiation entering into the energy meter, we use a cutoff filter. To measure energy of the laser pulse incident upon the sample, E_{inc}, we use a beam-splittter that directs a fraction of the laser beam onto another energy meter as shown in figure 1. Having measured E_{refl} and E_{inc}, the hemispherical total reflectivity, R, (a sum of specular and diffuse components of the reflected light) can be found as $R = E_{refl}/E_{inc}$. The incident laser fluence, F, is determined by dividing the incident laser pulse energy, E_{inc}, by the laser spot area on the sample. The total reflectivity is studied in a laser fluence range of 0.06–100 J cm^{-2}. After each laser shot, the studied sample is translated to a fresh spot on the sample. All experiments are performed in air of the atmospheric pressure. The studied metal is mechanically polished bulk titanium. After polishing the room-temperature reflectivity of titanium samples was measured at 1.06 μm and 0.69 μm wavelengths using a Perkin-Elmer Lambda 900 spectrophotometer with an integrating sphere. In this study, we also determine both surface damage and plasma ignition thresholds. The surface damage threshold is found as the lowest laser fluence that causes a surface damage to be visible under an optical microscope. The plasma ignition threshold is determined by detecting the onset of a bright violet flash from the irradiated spot using a photomultiplier with a filter that blocks the wavelengths longer 0.45 μm [29].

3. Results and discussion

The room-temperature reflectivity of our titanium sample measured with the Perkin-Elmer Lambda 900 spectrophotometer was found to be 0.58 and 0.51 at 1.06 and 0.69 μm wavelengths, respectively. These measured reflectivity values agree with reflectivity measurements of polished titanium reported in [30]. The damage thresholds were measured to be 0.9 and 0.8 J cm^{-2} at 1.06 and 0.69 μm wavelengths, respectively. The values of the plasma ignition threshold were found to be 1.2 J cm^{-2} ($\lambda = 1.06$ μm) and 1.1 J cm^{-2} ($\lambda = 0.69$ μm), which are slightly higher than those for the damage threshold. The similar relation between the damage and plasma ignition thresholds has been previously observed in nanosecond laser ablation of Al [29] and Mg [25]. The plots of the reflectivity of titanium as a function of laser fluence at studied laser wavelengths are shown in figure 2. These plots show that the reflectivity does not change with increasing laser fluence from about 0.06 to 1.3 at 1.06 μm and to 1.1 J cm^{-2} at 0.69 μm; and measured reflectivity values are noticeably different at the studied wavelengths. It is also seen that these reflectivity values agree with the room-temperature reflectivity values measured with the Perkin-Elmer Lambda 900 spectrophotometer. With further increasing laser fluence, the reflectivity at both wavelengths significantly drops and the spectral reflectivity difference decreases. Our experimental data show that within the experimental uncertainty the laser fluence values, at which the reflectivity begins to drop, correlate with those of the plasma ignition threshold. As seen from figure 2, there is almost no difference between $R(F)$ dependencies for the studied wavelengths at $F > 10$ J cm^{-2}.

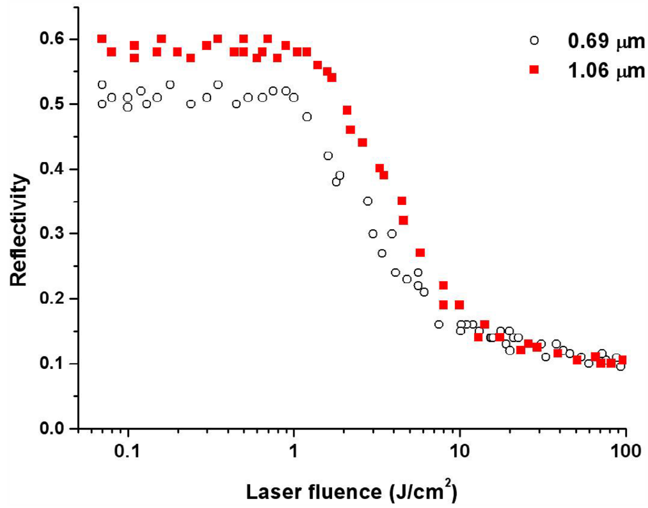

Figure 2. Reflectivity of titanium in nanosecond laser ablation of Ti at $\lambda = 1.06$ and 0.69 μm in air.

The reflectivity drop observed in our experiment can be caused by Drude's temperature dependence of the optical constants of a metal heated by the laser pulse [31, 32] and absorption of the laser beam in plasma generated in front of the irradiated sample [20, 22]. To understand Drude's temperature effect on the reflectivity drop of titanium, we computed the surface temperature, T_{surf}, of titanium at the damage threshold fluence for both wavelengths using the formula derived by Ready [33]

$$T_{surf}(t) = \frac{(1-R)\sqrt{a}}{k\sqrt{\pi}}\int_0^t \frac{I(t-\tau)}{\sqrt{\tau}}d\tau + T_0 \quad (1)$$

where a is the thermal diffusivity, k is the thermal conductivity, I is the intensity of the incident laser light, t is the time, T_0 is the initial temperature, and τ is the integration variable. The plots of the surface temperature computed using

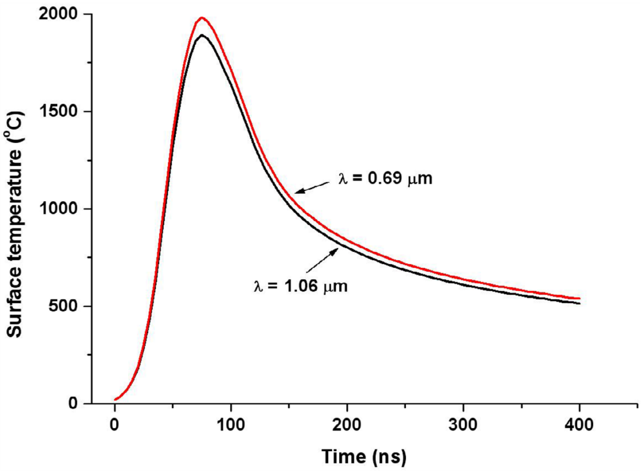

Figure 3. Surface temperature of the titanium sample as a function of time at the damage threshold laser fluence.

$k = 21.9$ W · m^{-1} · K^{-1}, $a = 9 \times 10^{-6}$ m^2 s^{-1}, $T_0 = 20$ °C, $R = 0.58$ at $\lambda = 1.06$ μm, and $R = 0.51$ at $\lambda = 0.69$ μm are shown in figure 3, where we can see that the maximum surface temperature is about 1890 °C at $\lambda = 1.06$ μm, and 1980 °C at $\lambda = 0.69$ μm.

These maximum surface temperature values computed at the damage threshold laser fluence are larger than the melting point of titanium (1670 °C). Thus, our reflectivity measurements and surface temperature estimations show that the reflectivity of the titanium sample does not change up to the temperature slightly above the melting point. We note that Drude's temperature effect on light reflection at some laser wavelengths has been theoretically studied in [31, 32], where the reflectivity decrease with increasing temperature has been predicted. The discrepancy between our observation and theoretical predictions can be explained by the fact that the theory is valid only for ideally polished and clean metal surfaces. For real surfaces, which are commonly contaminated, oxidized, covered with adsorbates, and have nano/microstructural defects, the Drude theory may not be well applicable as discussed in [28]. Since the reflectivity drop in our experiment begins at laser fluence only slightly above the damage threshold and correlates with the plasma ignition threshold, we believe that the observed reflectivity drop is caused by the plasma absorption effect. The reflection of the laser light under conditions of plasma generation has been first considered first in [22] and later in [34]. Figure 4 schematically shows the reflection process in this case. There are two types of laser-induced plasmas for ablation in air or any other ambient gas, namely, the plasma of ablated material and the ambient gas plasma. Depending on laser fluence, the ambient gas plasma can take a form of a laser-supported combustion wave or laser-supported detonation wave [35, 36].

Taking into consideration the laser beam absorption in the plasma, the time-integrated reflectivity is given by [22]

$$R = \left(\int_0^{\tau_L} I_0(t) R_s(t) \exp\left[-2\theta(t)\right] \mathrm{d}t \right) \Big/ \int_0^{\tau_L} I_0(t) \mathrm{d}t \qquad (2)$$

where $I_0(t)$ is the incident laser pulse power, t is the time, $R_s(t)$ is the reflectivity of the sample surface, $\theta(t)$ is the total

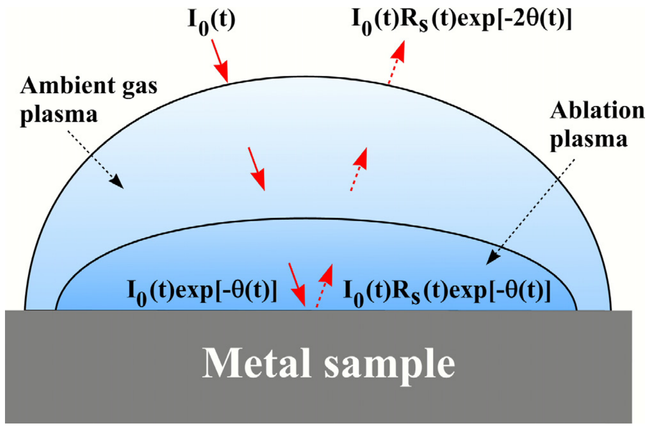

Figure 4. Schematics of laser-induced plasmas and reflection of the laser pulse from the sample-plasma system, where $I_0(t)$ is the incident laser pulse power, $I_0(t)\exp[-\theta(t)]$ is the laser pulse power that arrives at the sample surface, $\theta(t)$ is the total optical thickness of the plasma, $I_0(t)R_s(t)\exp[-\theta(t)]$ is the laser pulse power reflected from the sample surface, $R_s(t)$ is the reflectivity of the sample surface, $I_0(t)R_s(t)\exp[-2\theta(t)]$ is the laser pulse power that escapes the sample-plasma system.

optical thickness of the plasma, and τ_L is the laser pulse duration. The equation (4) shows that R depends on both the total optical thickness of the plasma θ and the surface reflectivity R_s.

In general, the total wavelength effect on the laser light reflection in ablation depends on both laser light absorption in surface layer of the sample and in the plasma. The reflectivity wavelength dependence of the surface layer is described by the Fresnel and Drude formulae [32]. For a smooth, flat, and clean surface the reflectivity is given by

$$R = \left| \frac{\varepsilon^{1/2} - 1}{\varepsilon^{1/2} + 1} \right|^2 = \frac{(n-1)^2 + k^2}{(n+1)^2 + k^2} \qquad (3)$$

where ε is the complex dielectric function, n is the refractive index and k is the extinction coefficient. For metals, ε is given by relation [37, 38]

$$\varepsilon(\omega) = 1 - \frac{\omega_p^2}{\omega(\omega - i\nu_{\text{eff}})}, \qquad (4)$$

where ω is the angular frequency of the laser light, $\omega_p = (4\pi n_e e^2/m_e)^{1/2}$ is the electron plasma frequency in the metal, n_e is the density of free electrons in the metal, e is the electron charge, m_e is the electron mass, $\nu_{\text{eff}} = \nu_{\text{e–ph}} + \nu_{\text{e–e}}$ is the effective collision frequency, $\nu_{\text{e–ph}}$ and $\nu_{\text{e–e}}$ are contributions of the electron–phonon and electron–electron collisions, respectively. In contrast to femtosecond laser pulses [38], the contribution of $\nu_{\text{e–e}}$ is small in the case of nanosecond laser pulses. The relations (3) and (4) predict the increase of the reflectivity with increasing light wavelength. Using table values of n and k for titanium from [39], equation (1) gives the reflectance of 0.624 and 0.615 at 1.06 μm and 0.69 μm, respectively. These calculated reflectance values are higher than those measured in our study ($R = 0.58$ at $\lambda = 1.06$ μm, and $R = 0.51$ at $\lambda = 0.69$ μm). Furthermore, these calculated reflectance values show a small spectral effect for the studied wavelengths. These discrepancies are explained by the fact that the table values of n and k were obtained for clean and smooth thin films of high optical quality, while the surface of our real sample is not ideal and has nano/microstructural defects, oxide film, and contaminants, which result in a more pronounced wavelength effect on the reflectance.

The absorption of the laser light in plasma has been previously modeled in [40–46]. At the studied laser wavelengths, the absorption of laser light in plasma occurs dominantly through inverse bremsstrahlung mechanism [42, 44, 46]. An analysis performed in [42] shows that the absorption coefficient of the laser radiation in the laser-induced plasma is approximately proportional to the square of the laser light wavelength, the square of the electron density, and to $T^{3/2}$. Experimentally, the absorption of the incident laser pulse in the plasma has been previously studied in [22, 40, 41] using a technique of a probe hole in the center of the irradiated spot. By measuring the intensity of laser light transmitted through the probe hole, this technique allows to find the intensity of the laser light that reaches the surface after attenuation in plasma $I_0(t)\exp[-\theta(t)]$ (see figure 4) and optical thickness of the laser-induced plasma. We note that the transient plasma can defocus the incident laser beam at high laser fluences [47], significantly complicating theoretical treatment of the laser light reflection.

At the present time, little is known about the reflectivity of the surface that undergoes ablation and is screened by the plasma (term $R_s(t)$ in equation (2)). For nanosecond laser pulses, ablation is dominantly driven by vaporization and phase explosion mechanisms, depending on laser fluence [41, 44, 48]. The phase explosion threshold for metals is in a range of about 5–15 J cm^{-2} [44, 49, 50]. Therefore, in our study, initially solid sample surface becomes liquid and can be further changed to a supercritical fluid state (no distinction between the liquid and vapor states). The optical properties of liquid metals have been previously studied in a number of works [51–53]. It has been shown that the reflection of light by liquid metals is well described by the Fresnel and Drude equations. A serious problem in modeling the reflection from the liquid layer produced in laser ablation is to take into account transient geometrical fluctuations of surface profile caused by ablation during laser pulse. For example, nanoscale transient ripples on the surface of the melted layer can significantly reduce the reflection due to plasmonic absorption, similar to the reduced reflection from solid-state surface nanostructures produced by laser pulses [54, 55], while microscale transient ripples can affect the reflectance through Fresnel angular dependence. The wavelength effect on Fresnel absorptivity of wavy molten metal surfaces has been modeled in [56] for CW CO_2 laser radiation. To our knowledge, there are no studies on optical properties of the transient nano/microripples induced on a metal surface melted by a nanosecond laser pulse.

When the surface layer temperature exceeds $0.9T_c$, where T_c is the critical temperature, the phase explosion mechanism comes into play [48]. The phase explosion effect on reflectivity drop has been observed by Kudryashov *et al* [57] in ablation of graphite by nanosecond KrF laser at intermediate laser fluencies. Wu and Shin [55] have theoretically calculated absorption coefficient of aluminum near the critical point at the wavelength of 532 nm using the Drude model and found that its value is smaller by about three orders of magnitude as compared with room temperature value. The wavelength effect on the absorption coefficient of aluminum near the critical point has been demonstrated in [59], where the absorption coefficient is predicted to decrease with increasing the laser wavelength.

The above discussion shows that laser light absorption in plasma increases, while the absorption in the surface layer decreases with increasing the laser wavelength. We believe that this fact plays a role in reducing the wavelength effect on the total reflection at $F > 10$ J cm^{-2} in our experimental data shown in figure 2.

4. Conclusions

In this work, we perform a comparative study on the reflection of nanosecond laser pulses with different wavelengths (1.06 and 0.69 μm) in ablation of titanium in air. Our experiments show that laser wavelength effect on reflection is essential at low laser fluence values, while it becomes negligible for laser fluence values exceeding the plasma threshold by about an order of magnitude. We speculate that the disappearance of the wavelength effect is explained by opposite actions of the laser light absorption in plasma that increases with the laser wavelength and absorption in the surface layer that decreases with the laser wavelength.

References

[1] Anisimov S I and Luk'yanchuk B S 2002 Selected problems of laser ablation theory *Phys.—Usp.* **45** 293–324
[2] Bäuerle D 2000 *Laser Processing and Chemistry* (Berlin: Springer)
[3] Phipps C R ed 2007 *Laser Ablation and its Applications* (New York: Springer)
[4] Li L, Hong M, Schmidt M, Zhong M, Malshe A, In'tveld B H and Kovalenko V 2011 Laser nano-manufacturing—state of the art and challenges *CIRP Ann.* **60** 735–55
[5] Gyorgy E, Perez del Pino A, Serra P and Morenza J L 2004 Influence of the ambient gas in laser structuring of the titanium surface *Surf. Coat. Technol.* **187** 245–9
[6] Bulgakova N M, Panchenko A N, Tel'minov A E and Shulepov M A 2010 Formation of microtower structures in nanosecond laser ablation of liquid metals *Appl. Phys.* A **98** 393–400
[7] Pedraza A J, Fowlkes J D and Guan Y F 2003 Surface nanostructuring of silicon *Appl. Phys.* A **77** 277–84
[8] Wang Z B *et al* 2004 Parallel nanostructuring of GeSbTe film with particle mask *Appl. Phys.* A **79** 1603–6
[9] Hendow S T and Shakir S A 2010 Structuring materials with nanosecond laser pulses *Opt. Express* **18** 10189–99
[10] Chrisey D B and Hubler G K (ed) 1994 *Pulsed Laser Deposition of Thin Films* (New York: Wiley)
[11] Zorba V, Boukos N, Zergioti I and Fotakis C 2008 Ultraviolet femtosecond, picosecond and nanosecond laser

microstructuring of silicon: structural and optical properties *Appl. Opt.* **47** 1846–50

[12] Tang G, Hourd A C and Abdolvand A 2012 Nanosecond pulsed laser blackening of copper *Appl. Phys. Lett.* **101** 231902

[13] Russo R E *et al* 2011 Laser plasma spectrochemistry *J. Anal. At. Spectrom.* **26** 1596–603

[14] Gottfried J L, De Lucia F C, Munson C A and Miziolek A W 2009 Laser-induced breakdown spectroscopy for detection of explosives residues: a review of recent advances, challenges, and future prospects *Anal. Bioanal. Chem.* **395** 283–300

[15] Ta D V *et al* 2015 Nanosecond laser textured superhydrophobic metallic surfaces and their chemical sensing applications *Appl. Surf. Sci.* **357** 248–54

[16] Ocana J L, Jagdheesh R and Garcia-Ballesteros J J 2016 Direct generation of superhydrophobic microstructures in metals by UV laser sources in the nanosecond regime *Adv. Opt. Technol.* **5** 87–93

[17] Gorny S G, Odintsova G V, Otkeeva A V and Veiko V P 2011 Laser induced multicolor image formation on metal *Proc. SPIE* **7996** 799605

[18] Kurella A and Dahorte N B 2005 Review paper: surface modification for bioimplants: the role of laser surface engineering *J. Biomater. Appl.* **20** 5–50

[19] Haverkamp J, Mayo R M and Bourham M A 2003 Plasma plume characteristics and properties of pulsed laser deposited diamond-like carbon films *J. Appl. Phys.* **93** 3627–34

[20] Basov N G, Boiko V A, Krokhin O N, Semenov O G and Sklizkov G V 1969 Reduction of reflection coefficient for intense laser radiation of solid surfaces *Sov. Phys.—Tech. Phys.* **13** 1581–2

[21] Dymshits Y I 1977 Reflection of intense radiation from a thin metal film *Sov. Phys.—Tech. Phys.* **22** 901–2

[22] Vorob'ev A Y 1985 Reflection of the pulsed ruby laser radiation by a copper target in air and in vacuum *Sov. J. Quantum Electron.* **15** 490–3

[23] Mao X and Russo R E 1997 Observation of plasma shielding by measuring transmitted and reflected laser pulse temporal profiles *Appl. Phys.* A **64** 1–6

[24] Benavides O, de la Cruz May L and Flores Gil A 2013 A comparative study on reflection of nanosecond Nd-YAG laser pulses in ablation of metals in air and in vacuum *Opt. Express* **21** 13068–73

[25] Benavides O, de la Cruz May L, Flores Gil A and Jimenez L J A 2015 Experimental study on reflection of high-intensity nanosecond Nd:YAG laser pulses in ablation of metals *Opt. Lasers Eng.* **68** 83–6

[26] Russo R E, Mao X L, Borisov O V and Liu H 2000 Infuence of wavelength on fractionation in laser ablation ICP-MS *J. Anal. At. Spectrom.* **15** 1115–20

[27] Vorobyev A Y and Guo C 2007 Femtosecond laser structuring of titanium implants *Appl. Surf. Sci.* **253** 7272–80

[28] Vorobyev A Y and Guo C 2011 Reflection of femtosecond laser light in multipulse ablation of metals *J. Appl. Phys.* **110** 043102

[29] Vorobyev A Y, Kuzmichev V M, Kokody N G, Kohns P, Dai J and Guo C 2006 Residual thermal effects in Al following single ns- and fs-laser pulse ablation *Appl. Phys.* A **82** 357–62

[30] Vorobyev A Y, Topkov A N, Gurin O V, Svich V A and Guo C 2009 Enhanced absorption of metals over ultrabroad electromagnetic spectrum *Appl. Phys. Lett.* **95** 121106

[31] Libenson M N, Romanov G S and Imas Y A 1969 Temperature dependence of the optical constants of a metal in heating by laser radiation *Sov. Phys.—Tech. Phys.* **13** 925–7

[32] Ujihara K 1972 Reflectivity of metals at high temperatures *J. Appl. Phys.* **43** 2376–83

[33] Ready J F 1971 *Effects of High-Power Laser Radiation* (New York: Academic)

[34] Tokarev V N, Lunney J G, Marine W and Sentis M 1995 Analytical thermal model of ultraviolet laser ablation with single-photon absorption in the plume *J. Appl. Phys.* **78** 1241–6

[35] Wen S B, Mao X, Greif R and Russo R E 2007 Laser ablation induced vapor plume expansion into a background gas. II. Experimental analysis *J. Appl. Phys.* **101** 023115

[36] Radziemski L J and Cremers D A (ed) 1989 *Laser-Induced Plasmas and Applications* (New York: Dekker)

[37] Born M and Wolf E 1980 *Principles of Optics* (Oxford: Pergamon)

[38] Kirkwood S E, Tsui Y Y, Fedosejevs R, Brantov A V and Bychenkov V Y 2009 Experimental and theoretical study of absorption of femtosecond laser pulses in interaction with solid copper targets *Phys. Rev.* B **79** 144120

[39] Johnson P B and Christy R W 1974 Optical constants of transition metals: Ti, V, Cr, Mn, Fe, Co, Ni, and Pd *Phys. Rev.* B **9** 5056–70

[40] Bulgakov A V and Bulgakova N M 1999 Thermal model of pulsed laser ablation under the conditions of formation and heating of a radiation-absorbing plasma *Quantum Electron.* **29** 433–7

[41] Bulgakova N M and Bulgakov A V 2001 Pulsed laser ablation of solids: transition from normal vaporization to phase explosion *Appl. Phys.* A **73** 199–208

[42] Ho J R, Grigoropoulos C P and Humphrey J A C 1996 Gas dynamics and radiation heat transfer in the vapor plume produced by pulsed laser irradiation of aluminum *J. Appl. Phys.* **79** 7205–15

[43] Autrique D, Chen Z, Alexiades V, Bogaerts A and Rethfeld B 2012 A multiphase model for pulsed ns-laser ablation of copper in an ambient gas *AIP Conf. Proc.* **1464** 648–59

[44] Marla D, Bhandarkar U V and Joshi S S 2014 A model of laser ablation with temperature-dependent material properties, vaporization, phase explosion, and plasma shielding *Appl. Phys.* A **116** 273–85

[45] Bogaerts A and Chen Z 2005 Effect of laser parameters on laser ablation and laser-induced plasma formation: a numerical modeling investigation *Spectrochim. Acta* B **60** 1280–307

[46] Phipps C R, Turner T P, Harrison R F, York G W, Osborne W Z, Anderson G K, Corlis X F, Steele H S, Spicochi K C and King T R 1988 Impulse coupling to targets in vacuum by KrF, HF, and CO_2 single-pulse lasers *J. Appl. Phys.* **64** 1083–96

[47] Danilov P A, Zayarnyi D A, Ionin A A, Kudryashov S I, Makarov S V, Rudenko A A, Yurovskikh V I, Kulchin Y N, Vitrik O B and Kuchmizhak A A 2014 Mechanisms of formation of sub- and micrometre-scale holes in thin metal films by single nano- and femtosecond laser pulses *Quantum Electron.* **44** 540–6

[48] Kelly R and Miotello A 1996 Comments on explosive mechanisms of laser sputtering *Appl. Surf. Sci.* **96–8** 205–15

[49] Porneala C and Willis D A 2006 Observation of nanosecond laser-induced phase explosion in aluminum *Appl. Phys. Lett.* **89** 211121

[50] Guillemot F *et al* 2004 Single-pulse KrF laser ablation and nanopatterning in vacuum of β-titanium alloys used in biomedical applications *Appl. Phys.* A **79** 811–3

[51] Smith N V 1967 The optical properties of liquid metals *Adv. Phys.* **16** 629–36

[52] Hodgson J N 1961 The optical properties of liquid indium, cadmium, bismuth, and antimony *Phil. Mag.* **7** 229–36

[53] Abeles F (ed) 1966 *Optical Properties and Electronic Structure of Metals and Alloys* (Amsterdam: North-Holland)

[54] Vorobyev A Y and Guo C 2005 Enhanced absorptance of gold following multi-pulse femtosecond laser ablation *Phys. Rev.* B **72** 195422

[55] Vorobyev A Y and Guo C 2013 Direct femtosecond laser surface nano/microstructuring and its applications *Laser Photon. Rev.* **7** 385–407

[56] Kaplan A F H 2014 Laser absorptivity on wavy molten metal surfaces: categorization of different metals and wavelengths *J. Laser Appl.* **26** 012007

[57] Kudryashov S I, Tikhov A A and Zvorykin V D 2011 Near-critical nanosecond laser-induced phase explosion on graphite surface *Appl. Phys.* A **102** 493–9

[58] Wu B and Shin Y C 2006 Absorption coefficient of aluminum near the critical point and the consequences on high-power nanosecond laser ablation *Appl. Phys. Lett.* **89** 111902

[59] Cao Y, Zhao X and Shin Y C 2013 Analysis of nanosecond laser ablation of aluminum with and without phase explosion in air and water *J. Laser Appl.* **25** 032002